Target Detection System in Sea Clutter Based on Simulated Radar Processing

Xia Wu
School of Electronics and Information Engineering, Tongji University, 201804, Shanghai, P. R. China

***Abstract* - In this paper, based on electromagnetic (EM) scattering theory, we present a target detection system in sea clutter working with simulated Synthetic Aperture Radar (SAR) images. A numerical case CVN-76 aircraft carrier was computed by using multilevel fast multipole algorithm (MLFMA). And the Fung and Lee sea-spectrum model was employed for three-dimensional wind driven ocean spectrum. Co-polarization and cross-polarization imaging results in L-band were generated through a fast back projection (FBP) algorithm by the given polarization, incident angle, wind speed and wind direction.**

***Index Terms* —EM scattering, target detection, sea clutter, SAR image, complex targets.**

1. Introduction

Research on target detection mechanism in clutter environments has attracted much attention, since monitoring and positioning of the aircrafts, fishing boats and warships in sea clutter play a significant role on the economy and defense in every country.

Most ocean wave spectra are based on an empirical or semi-empirical model, including, for example, Pierson-Moskowitz spectra [1], Fung and Lee sea-spectrum model [2] etc. In this work, we computed the EM scattering of electrically large targets by using multilevel fast multipole algorithm (MLFMA) [3]. For co-polarization (horizontal-horizontal (HH) and vertical-vertical (VV)), and cross-polarization (horizontal-vertical (HV) and vertical-horizontal (VH)), SAR imaging were generated by employing a fast back projection (FBP) algorithm [4].

2. Geometric modeling with CAD

A fast geometry-EM CAD modeling plays a key role to achieve computational electromagnetic algorithms.

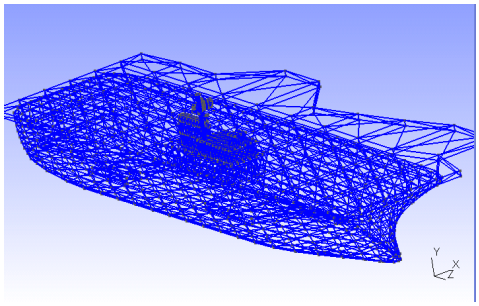

Fig. 1. 3D mesh of CVN-76 generated by Gmsh.

The USS Ronald Reagan CVN-76 aircraft carrier was selected as the target model in this paper. First, the geometry model was established by using Gmsh for initial meshes [5].

The CVN-76 model contains the main hull with deck equipment including bomb carts and forklifts. The original geometry version of CVN-76 is .obj which is provided for some 3DS application. Fig. 1 shows the mesh grids of CVN-76 generated by Gmsh.

The initial meshes contain 1766 nodes, 5268 edges and 3512 surface elements.

3. EM simulation

(1) Bistatic computation settings:

Then, we set the radar parameters, including the radar range resolution, the angle of incidence and azimuth. The scene receiver positions locate in the semicircle of the *xz*-plane (radius R = 4000 m, we selected 257 field points as receivers sketched in Fig. 2).

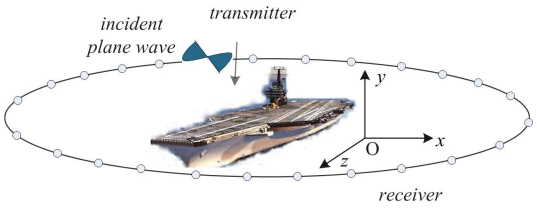

Fig. 2. The radar image mode scenario of CVN-76.

The incident plane wave (along the negative y direction as shown in Fig.2) is calculated as:

$$\vec{E}_i(r) = E_0 e^{j\vec{k}_i \cdot \vec{r}} \hat{e}_i \tag{1}$$

The local coordinate system (***h***, ***v***, ***k***) is as follows:

$$\vec{k} = k_i\left(\sin\theta_i\cos\phi_i\hat{e}_x + \sin\theta_i\sin\phi_i\hat{e}_y + \cos\theta_i\hat{e}_z\right) \tag{2}$$

$$\hat{h} = \frac{\hat{e}_z \times \hat{k}}{\left|\hat{e}_z \times \hat{k}\right|} = -\sin\phi_i\hat{e}_x + \cos\phi_i\hat{e}_y \tag{3}$$

$$\hat{v} = \hat{h} \times \hat{k} = \cos\theta_i\cos\phi_i\hat{e}_x + \cos\theta_i\sin\phi_i\hat{e}_y - \sin\theta_i\hat{e}_z \tag{4}$$

For a given transmitter position, and given frequency and polarization of transmission, the MLFMA with Message

Passing Interface [6] parallel EM simulation process is employed to compute and store the scattering field data.

Co-polarization (for HH polarization) radar images were generated through high-frequency electromagnetic scattering calculations and a fast back projection (FBP) algorithm for radar imaging, as shown in Fig. 3.

The bandwidth was chosen to be 1000 MHz (L-band, 1-2 GHz). Kaiser window function was introduced for the purpose of edge filtering with a fixed parameter (β =2.2) [7].

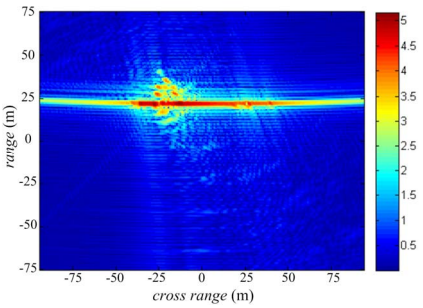

Fig. 3. HH polarization imaging of CVN-76 in L-band.

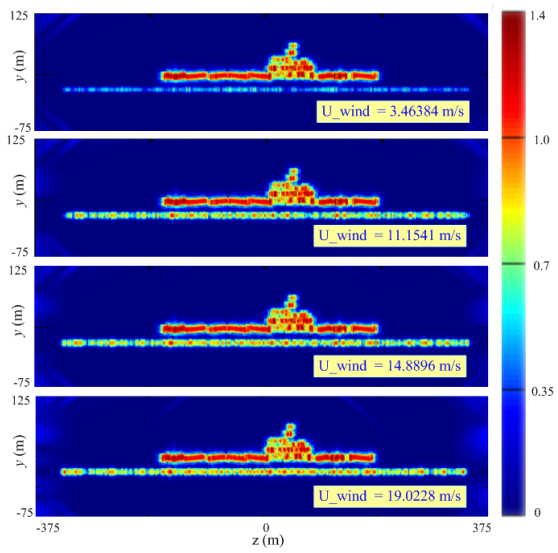

Fig. 4. Cross-polarization imaging of CVN-76 in L-band under different wind speed

(2) 3D dynamic sea surface modeling

The ocean spectrum was employed for three dimensional (3D) dynamic sea surface modeling. Hereby, a semi-empirical sea spectrum given by Fung and Lee [2] was employed as follows,

$$S(k,\phi)=\frac{1.4\times10^{-3}}{k^3}\exp(-\frac{0.74g^2}{k^2U\_wind^4})\Phi(\phi) \qquad (5)$$

where, $\Phi(\phi)=1+\left(1-e^{-sk^2}\right)\cos 2\phi$, and U_wind is the wind speed at the height z above sea surface:

$$U\_wind=\left(\frac{U*}{0.4}\right)\ln\left(\frac{z}{Z_0}\right) \qquad (6)$$

$$Z_0=\left(\frac{0.00684}{U*}\right)+4.28\times10^{-7}U*^2-0.000443 \qquad (7)$$

in which U^* is the friction velocity. Hereby, z =19.5 m.

Based on Fung and Lee sea spectrum, a complex object modeling was generated by the suitable interception of three-dimensional dynamic random rough sea surface with electrically large complex objects for numerical simulation. Electromagnetic simulation and imaging processing will be done on this new mesh grid.

With increasing wind speed of the sea surface, cross-polarization (for VH polarization) imaging results of the complex objects with CVN-76 and three-dimensional rough sea surface were demonstrated on Fig. 4, the wind direction was chosen to be 90 degrees.

4. Conclusion

A real-time numerical simulation scheme was proposed that combines raw radar data simulation, imaging and reconstruction of 3D electrically large complex targets in sea clutter. Consequently, the relationship between scattering properties and geometric structure could be established for target detection and classification. It provides a theoretical basis for fast 3D high-resolution image reconstruction as well.

Acknowledgment

This work was supported by the Shanghai Natural Science Foundation (Grant No. 16ZR1446300).

References

[1] Pierson W J, Moskowitz L. "A proposed spectral form for fully developed wind seas based on the similarity theory of S.A.Kitaigorodskii," *Journal of Geophysical Research*, vol.69, no.24, pp.5181-5190, 1964.

[2] A. K. Fung and K. K. Lee, "A semiempirical sea-spectrum model for scattering coefficient estimation," *IEEE J. Oceanic Eng.*, vol. OE-7, pp. 166-176, Oct. 1982.

[3] W. C. Chew, J. M. Jin, E. Michielssen, and J. Song, Fast and Efficient Algorithms in Computational Electromagnetics, Artech House, 2001.

[4] Samit Basu and Yoram Bresler, "O($N^2\log_2N$) filtered backprojection reconstruction algorithm for tomography," *IEEE Trans. IMAGE PROCESSING,* Vol. 9, No. 10, pp.1760-1773, Oct. 2000.

[5] Christophe Geuzaine and Jean-François Remacle. "Gmsh: a Three-Dimensional Finite Element Mesh Generator with Built-in Pre- and Post-processing Facilities," http://www.geuz.org/gmsh/ , May, 2004.

[6] Jean-Marc Adamo. "Multi-threaded object-oriented MPI-based message passing interface: the ARCH library," Boston : Kluwer Academic, 1998. ISBN 0792381653.

[7] J. F. Kaiser, "Nonrecursive digital filter design using the I_0 – sinh window function," *IEEE Int. Symp. on Circuits and Syst.,* San Francisco, CA, USA, pp. 20-23, Apr. 1974.